Chapter 2 – BACKGROUND

Strain gage measurements are the industry standard for determining the state-of-stress of a structure, quantifying airframe loads to evaluate if airframe load limits have been exceeded, or for calculating the remaining available airframe fatigue life. The foil strain gage is extremely accurate, reliable, economical, easy to use, exceptionally linear, highly repeatable, and possesses a very strong signal-to-noise ratio. As shown in Table 2-1, strain and temperature measurements are the most basic of all structural parameters and can be used to quantify many types of airframe failures (W. Sheppard, "SHM Flight Test Panels, Sensor Integration, Rev 3", project files, 2002).

Table 2-1: Strain and Temperature Measurements as Critical Health and Usage Monitoring Parameters.

Failure Mode	Structural Health Monitoring Sensor
Leaks	Gas detection/temperature
Disbond/delaminations	Strain/temp/acousto-ultrasonics/acoustic emission
Thermal protection failure	Strain/temperature
Overloads	Strain
Over pressure	Strain/pressure
Thermal damage	Temperature / strain / gas detection
Dynamic overloads	Acceleration / dynamic strain
Impact damage	Acoustic emission/train
Moisture/corrosion	Humidity sensor

The major drawbacks of conventional strain and temperature sensor technology are with its heavy wire weight, large bundle sizes, and that the technology provides only local measurements in very near proximity to the sensing region. Advanced sensing technology, such as distributed Bragg grating sensors, avoids some of the limitations of conventional measurements by providing enormous numbers of engineering parameters, such as strain, temperature, and structural shape, with a minimal weight penalty that cannot be matched by any other current sensing technology. Fiber optic sensors also have a safety advantage because they are chemically inert and, unlike conventional sensors, are immune to electromagnetic interference and are not susceptible to sparking or Joule heating. Because of their small size, these sensors can also be embedded within composite materials. Additional references to fiber optic sensing, smart structures, and fiber optic structural health monitoring can be found in the literature. [1-5]

2.1 MERITS OF FIBER OPTIC SENSORS

2.1.1 Weight

The primary reason for the popularity of fiber optic sensors resides in their weight. They are extremely light and are about the size of a human hair. This is an especially attractive feature for the aerospace community, where weight is crucial to mission and/or commercial success. As an example, Figure 2-1 shows a comparison between a typical strain gage installation and an analogous fiber optic sensor. In this example, the strain gage sensor itself is heavier and for most installations requires three copper lead wires to connect to

the data acquisition system. As will be explained in the next section, hundreds of fiber optic sensors can be located on one optical fiber. Therefore, considerable weight savings can be gained based on the sensor-to-sensor comparison as well as the sensor-to-lead wire efficiency gained by the fiber optic sensor. A typical installation is 0.1 to 1% the weight of conventional gage installations (based on past trade studies).

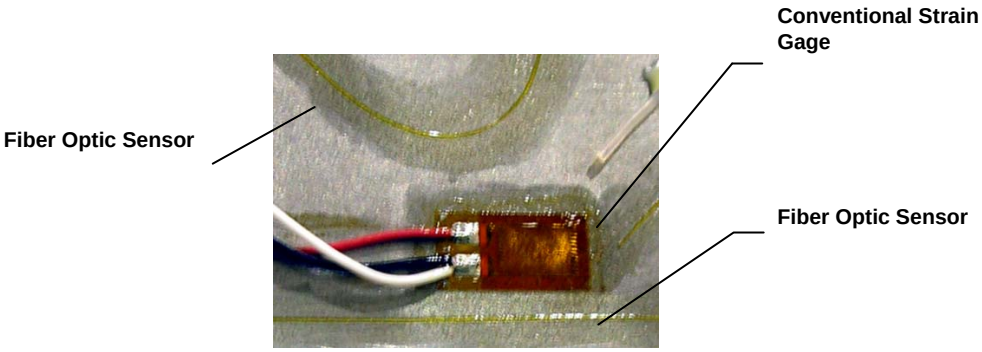

Figure 2-1: Comparison of Typical Installations of Strain Gages, and a Fiber Optic Sensor.

This comparison becomes even more dramatic when one compares the state-of-the-art for conventional high temperature metallic strain gages with an equivalent fiber optic sensor (Figure 2-2). For aerospace applications these weight savings have direct correspondence to increases in payloads that vehicles can deliver, and significantly extend the range at which they can travel.

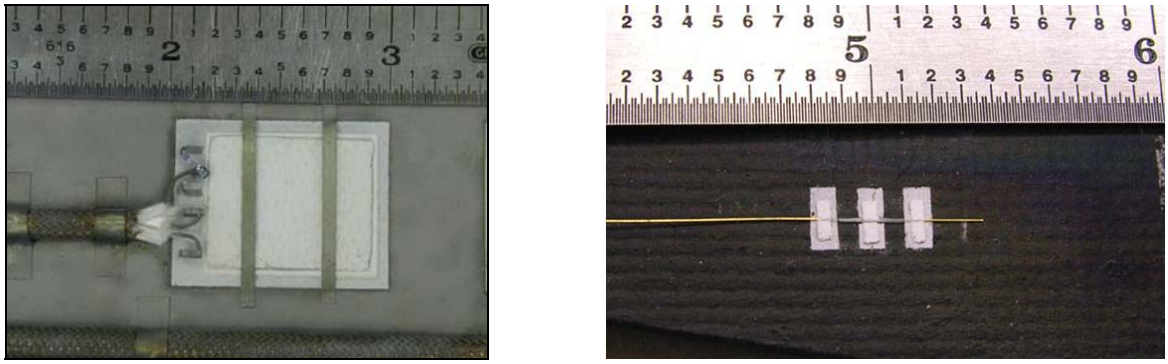

Figure 2-2: Comparison of Typical High Temperature Installations of a Strain Gage (Left), and a Fiber Optic Sensor (Right).

2.1.2 Multiplexing

In an industry where weight alone can be sufficient justification to incorporate a new technology, weight is only a small part of the Fiber Bragg Gratings (FBG) advantage. The real strength of the FBG resides in its capability to be multiplexed serially. This means that a single optical fiber can contain thousands of discrete FBG sensors along its length using the Optical Frequency Domain Reflectometry (OFDR) multiplexing scheme. For example, a recent flight test program at NASA Dryden conducted on a Predator-B (General Atomics Aeronautical Systems, Incorporated, San Diego, California) successfully flew a FBG system with six optical fibers, each containing approximately 500 fiber optic sensors. [6] Each of these sensors produced a measurement every 0.5 inch that was analogous to the discrete measurement provided by a strain gage at a fraction of the weight.

Multiplexing also provides benefits by dramatically reducing sizes of cable bundles and reducing the complexity of integration and testing of large-scale structural components. Figure 2-3 shows a dramatic comparison between conventional sensors and FBG technology for a ground test article and a flight test fixture. The flight test fixture was instrumented with both conventional and fiber optic sensors and flown at NASA Dryden Flight Research Center. [7] Lead wires from 32 strain gages are shown next to 5 optical fibers containing the same number of fiber optic sensors. (The strain gage instrumentation is shown as white and red jacketed lead wires, and the 5 optical fibers are visible on the left in purple.) This multiplexing advantage saves considerable amounts of time required for pre-flight installation, integration, and identification and trouble-shooting.

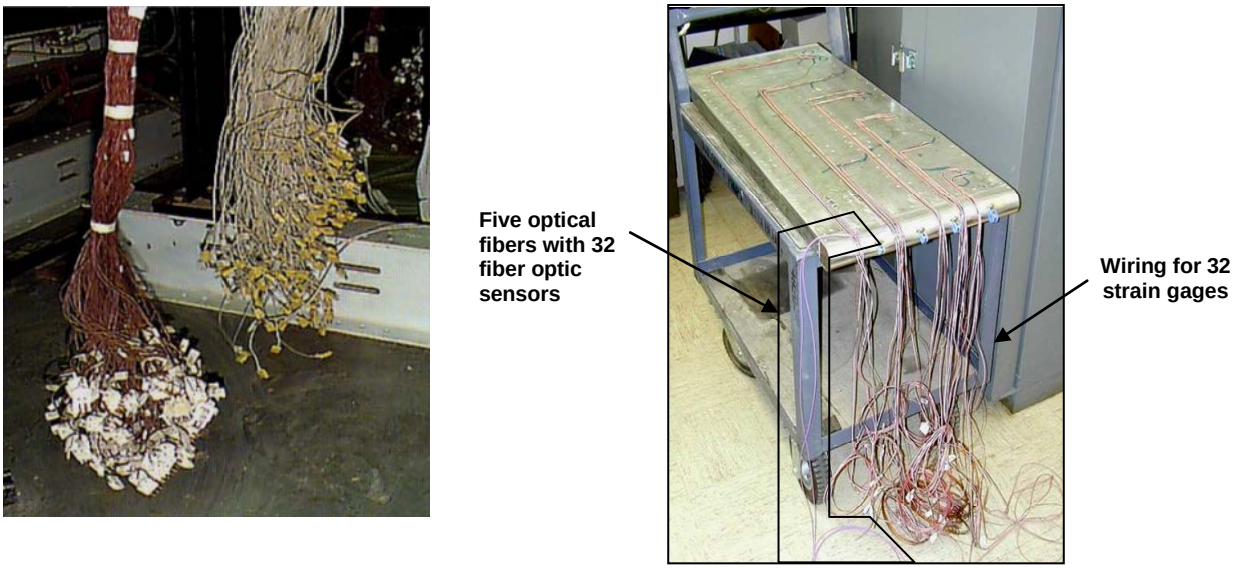

Figure 2-3: Instrumentation Comparison Between Strain Gage and Fiber Optic Sensor Technology.

2.1.3 Embedment

In addition to what has been mentioned previously about the small size of fiber optic sensors, this advantage means that it is more readily embedded within advanced composite materials. By inspection the cylindrical shape of the fiber sensor is clearly more conducive to embedding with composites because of its smooth non-intrusive geometry. This physical characteristic enables internal strain field measurement of complex material systems during the manufacturing process and testing. Figure 2-4 (left) shows a strain plot of FBG sensors embedded under the load-introduction device on the composite crew model structure called the CM-ALAS. The strain fields measured under the bolted joint were correlated with finite element predictions. Figure 2-4 (right) shows a composite shear panel during testing. This panel had 16 embedded fiber optic sensors that could be correlated with conventional sensors on the front and back of the structure.

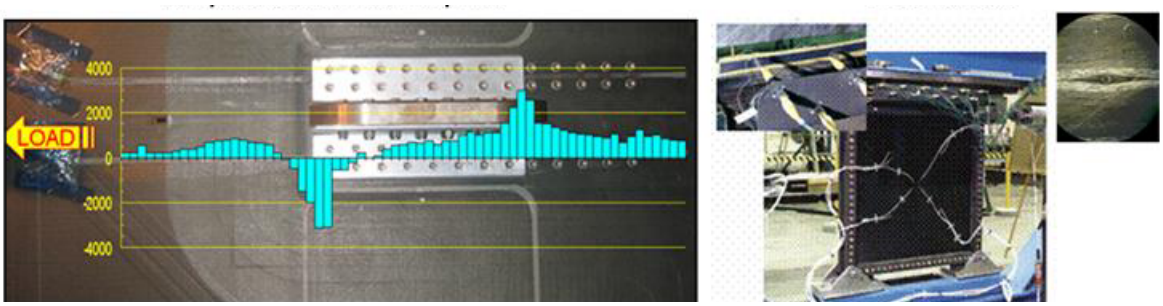

Figure 2-4: FBG Sensors Embedded in Composite Structures. Strain measurements from FBGs embedded under bolted joint on the composite crew module panel (left), and fiber optic sensors embedded in 2 ft by 2 ft shear panel (right).

The ability to embed has also led to technical challenges that have limited its application to aerospace structures. The issue of fiber ingress/egress from the composite has created technical challenges, which are the subject of ongoing research and development tasks. The measurement interpretation of embedded FBGs also hampers its acceptance. [8, 9] Interpreting measurements from FBGs embedded in composites is a multi-disciplinary problem. Expertise in sensor and measurement technology, structural mechanics, experimental stress analysis, composite materials, interrogation systems, and optics are all required to adequately understand these measurements while acquired from within complex materials systems.

2.1.4 Safety

Fiber optic sensors are also inherently safer than conventional sensors. Hermetically coated glass is chemically inert, not susceptible to corrosion, and does not have potential for ground loops, electrical faults, sparking, or Joule heating. These sensors also are not negatively impacted like common aircraft avionics systems with reactions to Electro-Magnetic Interference (EMI) or Electro-Magnetic Pulses (EMP).

2.2 FBG THEORY

Fiber Bragg Gratings (FBG) are produced in optical fibers, which consist of a silica glass cylindrical shaped core, surrounded by a silica cladding of slightly higher index of refraction, and a protective coating. The differences in indices of refraction between the core and the cladding create a waveguide, which as the name implies, serves to efficiently guide light waves down the core of the fiber.

FBGs are created by exposing an optical fiber to an ultraviolet interference pattern, which produces a periodic change in the core index of refraction. [10] These periodic changes cause a reflection when the light in the waveguide is of a particular wavelength while other wavelengths are transmitted in the fiber, as shown in Figure 2-5. The particular reflected wavelength, known as the Bragg wavelength (λ_B) is dependent upon the FBG's period of core index modulation (Λ) and the effective core index of refraction (n_0).

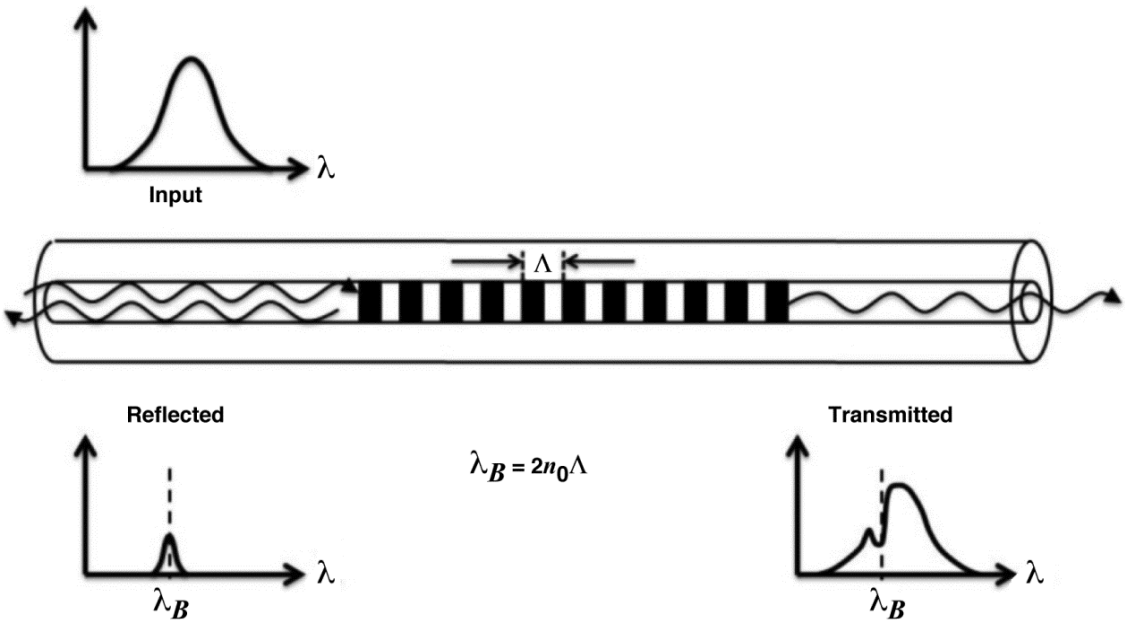

Figure 2-5: Reflected and Transmitted Light Through a Bragg Grating.

When the FBG is strained along the fiber axis, the Bragg grating stretches or contracts, causing Λ and n_0 to increase or decrease. This, in turn, produces an increase or decrease (i.e. δ) in λ_B directly related to Λ and n_0 as represented in equation (1).

$$\delta\lambda_B = \delta\left(2n_0\Lambda\right) = 2\Lambda\left(\delta n_0\right) + 2n_0\left(\delta\Lambda\right) \tag{1}$$

Assuming the strain is constant along the length of the Bragg grating, the change in Λ relates to the kinematic stretch of the fiber and in turn, relates to strain. The relationship between strain and change in index of refraction is determined using a strain-optic tensor comprised of photoelastic coefficients. The number of independent coefficients in the strain-optic tensor is reduced under the assumption that the fiber is optically isotropic, and the set of equations collapses to a single expression shown in equation (2) when the strain field is predominantly uniaxial along the fiber-grating axis.

$$\left[\frac{\Delta\lambda_B}{\lambda_B}\right] = \left(1 - p_e\right)\varepsilon + \left(\alpha_\Lambda + \alpha_n\right)\Delta T \tag{2}$$

where $\Delta\lambda_B$ is the change in Bragg wavelength, λ_B is the unstrained Bragg wavelength, p_e is a reduced, first order strain-optic coefficient, ε is the strain in the fiber direction, α_Λ is the coefficient of thermal expansion of the fiber, and α_n is the thermal-optic coefficient. Temperature measurements are made with FBGs by decoupling the strain field from the substrate by placing the fiber in a small tube and attaching the tube to the substrate. The tube allows the FBG to freely expand in the tube during loading. In this case, all terms but $\alpha_n\Delta T$ on the right side of the equation are zero. Pure mechanical strain is determined by bonding the FBG directly to the substrate and employing conventional temperature correction techniques established for strain gages. [11]

A typical optical fiber used in our research is single-mode with a cladding diameter of 127 µm and polyimide coating thickness of 7 µm. Each optical fiber contained multiple FBGs equally spaced with Bragg wavelengths of approximately 1546 nm and strain-optic coefficients, p_e, of 0.1667.

2.3 OPTICAL FREQUENCY DOMAIN REFLECTOMETRY

The system used at NASA Dryden is based on the Langley method using OFDR to interrogate FBG. Typical OFDR systems interpret a beat frequency between a reference arm and the sensing arm where the Device Under Test (DUT) is located; usually the interfering signal is generated through a Michelson interferometer. Figure 2-6 is a schematic of a typical OFDR system in a Michelson interferometer, composed of a wavelength-tunable laser (wavelength-swept laser) at ~1550 nm, a square-law photodiode detector, and two broadband reflective mirrors.

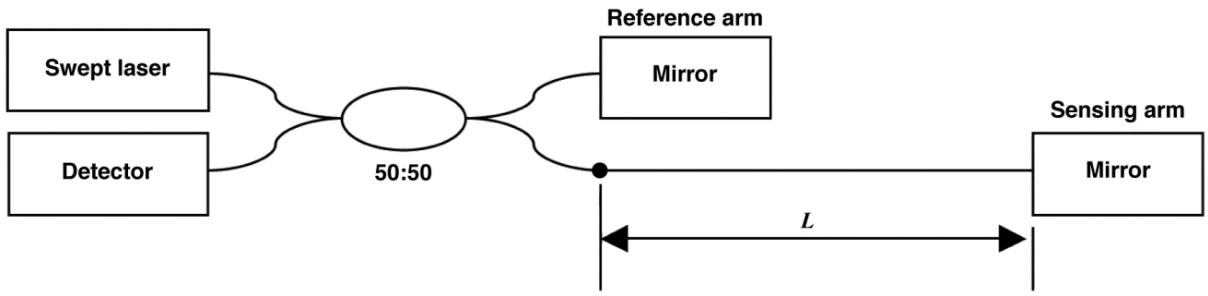

Figure 2-6: Schematics of a Typical OFDR System.

First, a tunable laser acts as a probe signal by continuously sweeping a predetermined frequency range. Light then travels through a 50:50 (2 x 2) fiber coupler, where light of equal intensity will then be reflected from each arm by a broadband reflector (mirror). Signals from both arms will be recombined by the fiber coupler; however, there is a corresponding phase difference (delay) between the reference arm and the sensing arm due to the path length difference L. The combined signal will interfere with one another due to this phase difference, where the intensity of the interfering signal will then be detected by the photodetector.

This same interference effect is applied to Bragg gratings used as strain sensors (Figure 2-7). In OFDR application of these sensors, the distance of each sensor can be individually determined first through sampling of output intensity while sweeping the laser's wavelength at all wavelength ranges. The output intensity/signal is a summation of the complete set of gratings located along the fiber length. Each grating is modulated with its unique frequency, a frequency that is determined by the grating's unique position on the fiber. These sensors are attached to an optical network for inspection.

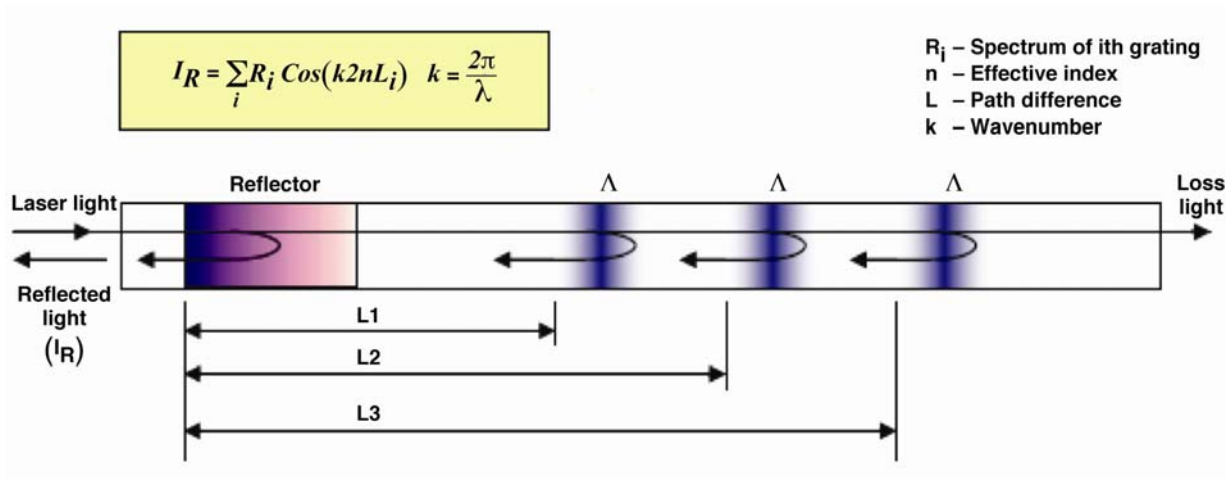

Figure 2-7: Fiber with Multiple Bragg Gratings.

Figure 2-8 illustrates the implementation of an optical network used to interrogate 4 fibers simultaneously. The tunable laser provides excitation for both the sensing and reference part of the network with 95% of its light to be partitioned equally among the four sensing arms. The remaining 5% is sent into a Michelson interferometer to generate a necessary sampling clock by which the four sensor arms are sampled.

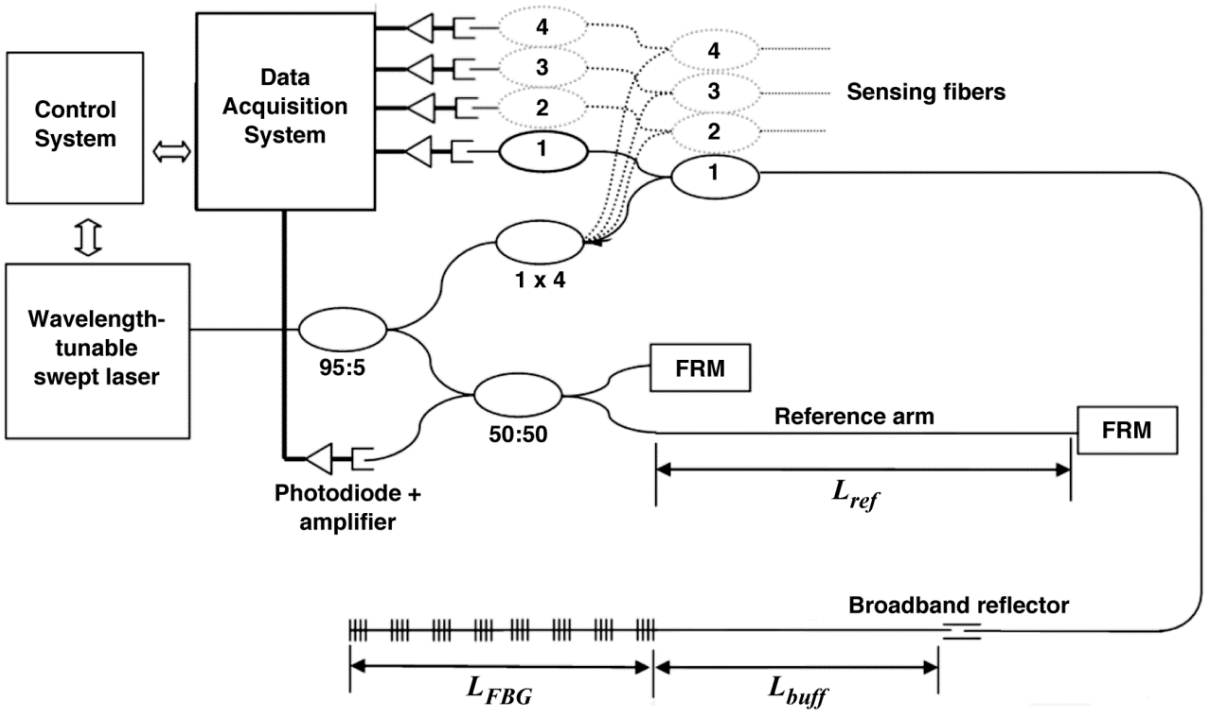

Figure 2-8: Fiber Optical Network with Reference Arm.

Applying Fourier transform to the intensity information gathered from the wavelength sweep range, this information is then mapped from wavelength domain to spatial domain (Figure 2-9). From the spatial domain each corresponding reflection represents each grating at its unique distance. Since applied strain detected from each FBG is linear to its shift in resonant wavelength, each grating's wavelength can be determined by taking the inverse Fourier transform from the spatial domain back to the wavelength domain, where the resonant wavelength change can be monitored (Figure 2-10).

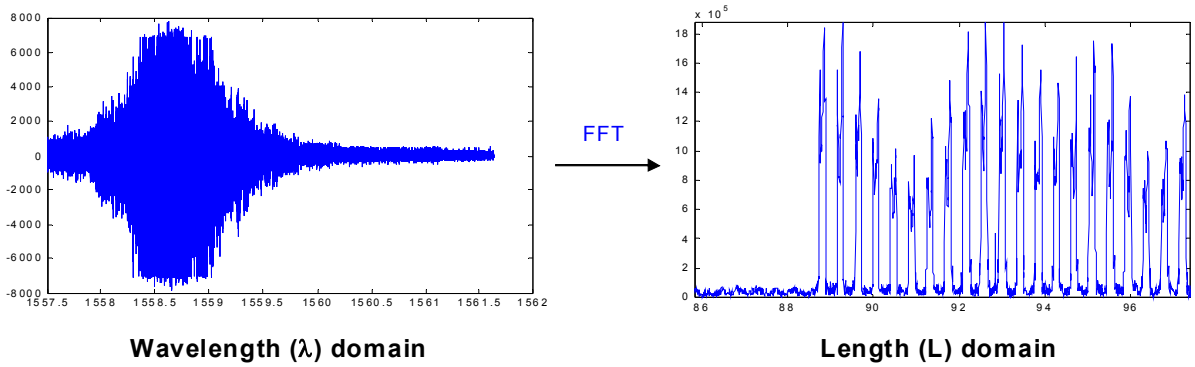

Figure 2-9: Fourier Transform from Wavelength to Spatial Domain to Discern Between Gratings.

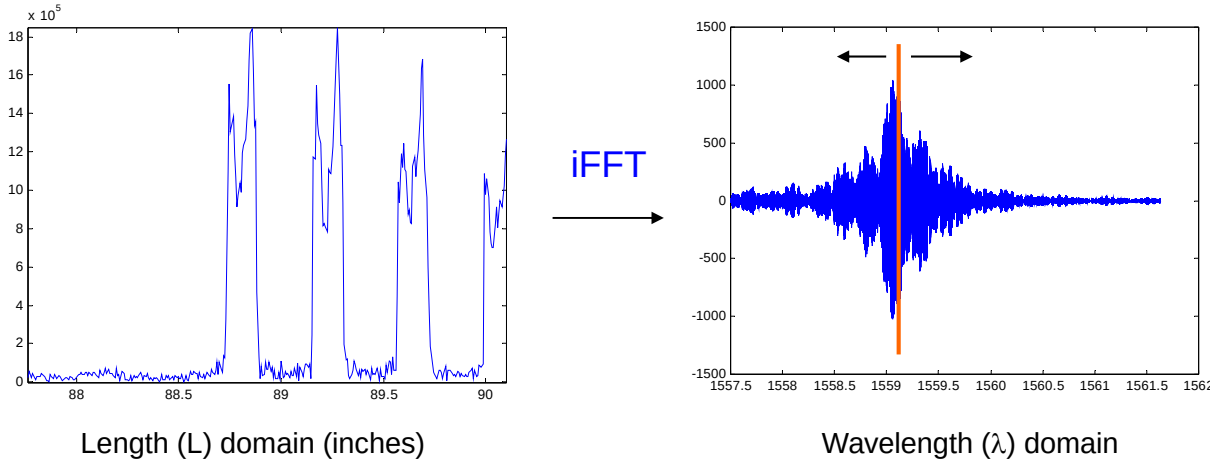

Figure 2-10: Window Function and Inverse Fourier Transform from Spatial to Wavelength Domain.

Applying this algorithm to real-time applications, where sample rates greater than five samples per second (sps) are needed, has proven to be limiting as a result of the initial Fourier transform. For applications requiring faster acquisition times, NASA Dryden has developed a method that yields acquisition speeds in excess of 60 sps. Recent advances in processing schemes, both in hardware and software have increased the sample rates of these systems to greater than 100 sps.